Journal of Engineering Science and Technology
Vol. 15, No. 5 (2020) 2939 - 2949

SIMULATION MICRORING RESONATOR BASED ON RACETRACK-SHAPED CONFIGURATION FOR GLUCOSE SENSING

ANANDA ARANSA[1], LILIK HASANAH[1], CAHYA JULIAN[1], RONI SUMANTRI[1], HARBI SETYO NUGROHO[1], AHMAD AMINUDIN[1], ROER EKA PAWINANTO[2], AHMAD RIFQI MD. ZAIN[3], SITI KUDNIE SAHARI[4], BUDI MULYANTI[2,*]

[1]Departemen Pendidikan Fisika, Universitas Pendidikan Indonesia, Jl. Dr. Setiabudhi no.229, Bandung 40154, Indonesia.
[2]Deparetmen Pendidikan Teknik Elektro, Universitas Pendidikan Indonesia, Jl. Dr. Setiabudhi no.229, Bandung 40154, Indonesia
[3]Institute of Microengineering and Nanoelectronics, Universiti Kebangsaan Malaysia, Bangi, Selangor 43600, Malaysia
[4]Faculty of Engineering, Universiti Malaysia Sarawak, Jalan Datuk Mohammad Musa, 94300 Kota Samarahan, Sarawak, Malaysia
*Corresponding author: bmulyanti@upi.edu

Abstract

The aim of our study is to increase the sensitivity of microring resonator using racetrack-shaped configuration for glucose sensing. We used glucose with various concentrations in 0-180 g/l range as analytes. Lumerical mode solutions used to simulate device. We obtained the sensitivity of racetrack-shaped resonator 79.7 nm/RIU. Basic add-drop configuration was used as the comparison, the sensitivity of racetrack-shaped resonator (79.7 nm/RIU) higher than basic add-drop resonator (70.32 nm/RIU). Coupling length reduces cavity loss, so that increase the performance of microring. The racetrack-shaped resonator configuration is suitable for glucose sensing and shows better performance than basic add-drop resonator.

Keywords: Glucose, Racetrack-shaped configuration, Sensitivity.

1. Introduction

Chemical detection of analysing chemicals at various concentration plays an important role in many areas [1]. There are several applications such as clinical analysis, healthcare, environmental monitoring and controlling in food industry [2]. In realizing good sensors for chemical detection/biosensing, required device that have a good limit detection. Sensors that work based on changes in the refractive index is among the most broadly utilized ways to recognize biochemical interaction. Integrated photonic device is a device that works by detecting changes in the refractive index, it offers several advantages including compact, quick response, easy fabrication, low cost, low power consumption, better limit detection. Microring resonator (MRR) is one of Integrated photonic device [3].

MRR has pulled in high interests as a result of their compact size, flexible structures. MRR consists of at least two waveguides that interact with one other at very small distances, straight waveguides serve as evanescence wave input and output couplers, while ring waveguide acts as the wavelength selective element. These devices offer a various advantage such as reducing the device size which affect to amount of analytes that needed for detection. Meanwhile, the reduction of size does not reduce the capability in sensing (sensitivity) [2].

The performance of MRR is indicated by Q-Factor and Free Spectral Range (FSR) which highly dependent from the geometries of MRRs such as radius, cross-section, a gap of the MRRs**.** A smaller cross-section would allow a higher evanescent field outside the waveguide and at the same time, the waveguide losses would increase**.** The large Q-Factor and FSR make the device has high sensitivity and a very small concentration of molecular detection capabilities [4]. There are various configurations on microring resonators such as basic-ring resonators with single waveguides, basic-ring resonators with double waveguide, racetrack-shaped resonators, double coupled resonators, serially coupled double ring resonators, parallel-coupled double ring resonators, and others. In each of the different configurations, the resulting performance varies due to the different geometries that affect the propagation of electromagnetic waves [5]. In solving complex Maxwell equations for electromagnetic, the Finite Difference Time Domain (FDTD) has widely used. Various applications were solved by FDTD due to the versatility of this method, for example optical devices, antennas, waveguide, radar cross-section, wave propagation, antenna design, discrete scattering studies, medical studies [2]. FDTD methods offer various advantages such as provide an accurate result, shorter solution time [1, 6]. Several studies investigating the performance of MRR have been carried out both in simulation and experiment.

Several studies have been reported previously. Ciminelli et al. [3] have reported the simulation results with the 3D FDTD method for basic add-drop ring resonator, however method that used consume time. The performance of MRRs for racetrack-shaped resonator configuration was based on experiment [5]. In this paper, we simulate two microring configuration models for biochemical sensing using FDTD methods, given by analytes with various concentrations. We simulated both configurations using Lumerical software mode solutions and compare both performances. The main purpose of this work is to increase the sensitivity of microring using racetrack-shaped configuration.

2. Theory

2.1. Microring parameter

Good performance is required to realize a device suitable for biochemical sensing. MRR performance depends on its geometry, there are several parameters determine it, Q-Factor, FSR, finesse, FWHM [4]. FWHM is the half resonance width which is defined as the full width at half maximum (FWHM) [7]. FWHM becomes very important in improving device performance. Based on the theory and experiments that have been carried out, both of them have explained that the limit of detection (LOD) depends on FWHM. i.e. LOD∝ (FWHM) [1]. FWHM can be expressed mathematically by Eq. (1) [8].

$$FWHM = 2\delta\lambda = \frac{\kappa^2\lambda^2}{\pi L n_{eff}} \quad (1)$$

FSR is the free spectral range of the resonator's response. FSR defined as the distance between adjacent resonance wavelength (Fig. 1) [4, 7]. A large FSR is required to get better sensing performance because wider FSR provides wider detection range [4]. FSR can be expressed by Eq. (2) [9].

$$FSR = \Delta\lambda = \frac{\lambda^2}{n_g L} \quad (2)$$

where n_g as group index and L as roundtrip of the length. From the equation, we can infer that FSR is inversely proportional to the size of the ring.

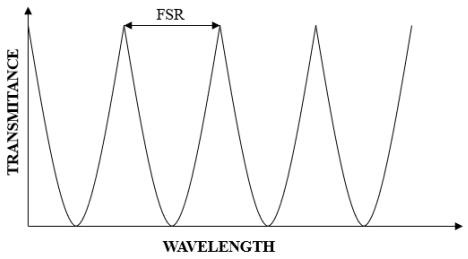

Fig. 1. Visualize of FSR.

The ratio of *FSR* and *FWHM* was defined as finesse, Eq. (3) [8].

$$F = \frac{FSR}{FWHM} \quad (3)$$

The *Q*-Factor is a parameter related to finesse [8]. *Q*-factor is defined as a measure of frequency structure sensitivity [7]. Represents the ratio of energy stored to energy lost in each cycle represents physical meaning of Q-Factor [4]. A large *Q*-Factor indicates that the energy lost is lower and the FWHM value is smaller.

$$Q = \frac{\lambda_{res}}{FWHM} = \frac{n_{eff}L}{\lambda}F = \frac{\pi n_{eff}L}{\lambda\kappa^2} = \frac{2\pi^2 n_{eff}R}{\lambda\kappa^2} \quad (4)$$

We see from Eq. (4) that *Q*-Factor is inversely proportional to FWHM, this is following with things that have been described before. A large *Q*-factor makes devices to have a smaller limit detection capability [10], so with a large *Q*-Factor, the smaller refractive index values can be detected.

We can be obtained a large *Q*-Factor by enlarging the radius of the ring (R_c), however R_c values are limited to sufficient FSR value. In addition to which have been previously mentioned *Q*-Factor influenced by losses in the cavity, to reduce losses in the cavity is an important thing [4].

2.2. Sensing mechanism

There are two main sensing mechanisms in microring resonator, surface mechanism sensing and homogeneous sensing both of which cause a resonance wavelength shift. On surface sensing mechanism molecules adsorb on a sensor surface which can be modeled as an ultrathin film (Fig. 2(a)). On homogeneous sensing mechanism, the analyte spreads to the aqueous medium in the top cladding, the molecule does not interact directly with the surface of the device (Fig. 2(b)). The optical roundtrip length of the ring affected the resonance of the ring, and the losses accumulated (all loss mechanisms combined, including coupling to bus waveguides) [4]. Resonance wavelengths shifting $\Delta\lambda_{res}$ are caused by changes in the effective index of the resonance mode n_{eff}, Eq. (5) [9, 11].

$$\Delta\lambda_{res} = \frac{\Delta n_{eff} L}{m}, m = 1, 2, 3 \ldots \quad (5)$$

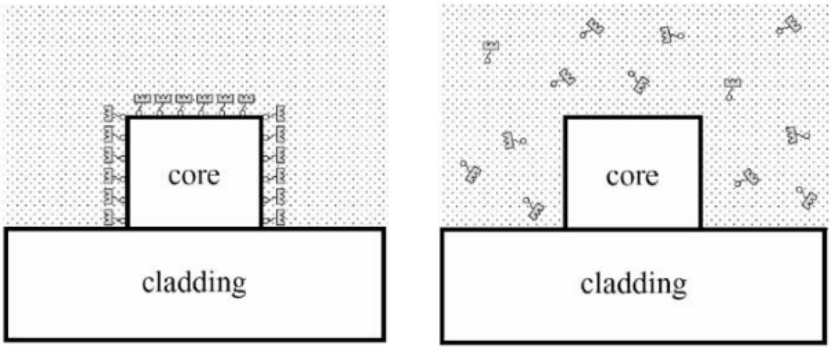

(a) (b)

Fig. 2. (a) surface sensing where molecule analytes absorb on the surface of device (b) homogeneous sensing where analytes exist in top cladding and spread in aqueous solution (adopted from literature [6]).

The change in the effective index of the resonance mode is affected by changes in the index of refractive effective in the top cladding, which is highly dependent on the sensing mechanism. Microring sensitivity depends on the *Q*-Factor on the micro-ring itself. Effective index changes are obtained by measuring shifting in resonance wavelengths. According to the resonance condition, we can write $\delta n_{eff}/n_{eff} = \delta\lambda_c/\lambda_c \propto 1/Q$, based on these things we can imply that to get a minimum effective index detected a high *Q*-Factor is required [10]. the sensitivity of devices can be calculated using Eq (6).

$$S = \frac{\partial\lambda_{res}}{\partial n_{eff}} \quad (6)$$

Another thing that needs to be considered is the detection limit, previously mentioned that devices that are well used as biochemical sensing need to have a very small detection limit. The detection limit is typically defined as the smallest detectable change of the waveguide parameters caused by analytes defined as detection limit which is related to the smallest amount of analyte that can be detected by microring [12]. The definition of sensitivity implies that the detection limit is then proportional to $\delta\lambda_c/S$, where $\delta\lambda_c$ is the detectable of wavelength shift [4].

3. Materials and Method

3.1. Design Model

We proposed a microring design based on a basic add-drop resonator and racetrack-shaped resonator configuration, this is based on previous research done by several researchers. The model that we used based Basic-add drop configuration on has a ring radius R = 500 microns, gap (G = 205 nm), and cross section 550 nm x 220 nm. As for the material used is Silicon (Si) on the waveguide and SiO_2 on the substrate. The glucose concentration was varied in the solution with a range of 0-180 g/l with an increase of 20 g/L at a wavelength of 1550 nm so that the shifting would then be used to obtain the sensitivity of the device. This model is used as comparison for racetrack-shaped resonator configuration.

In racetrack-shaped resonator configuration, we inspired to use racetrack-shaped resonators as a biochemical sensing configuration and characterized the device based on experiments. Radius, gap, and cross-section on the device used in this configuration are the same as the previous configuration, but there is one difference that is coupling length. in this configuration, the coupling length (L_c) used is 3 microns (in the previous configuration 0 microns. We used this model for glucose sensing in order to obtain better performance than the previous model which indicate by sensitivity.

The parameters in the design model that we used to simulate in detail are shown in Table 1. SOI (Silicon On Insulator) is the material that we used which offer various advantage, low-cost, high refractive index contrast, and high performance. The design of the model that we proposed to be simulated is shown in Figs. 3 and 4.

Table 1. Parameter of MRRs design model.

Parameter	Symbol	Unit	Model 1	Model 2
Coupling length	L_c	µm	0	3
Gap	G	µm	205	205
Radius	R	µm	5	5
Base-Width	W	µm	500	500
Height	h	µm	220	220

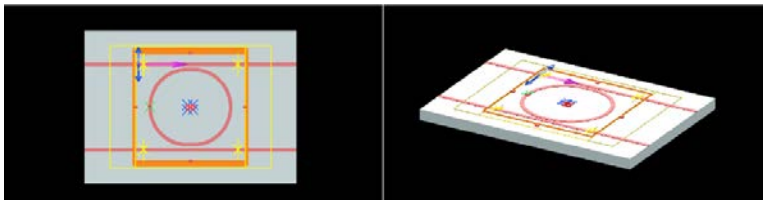

Fig. 3. Basic add-drop resonator view on XY and XZ axis.

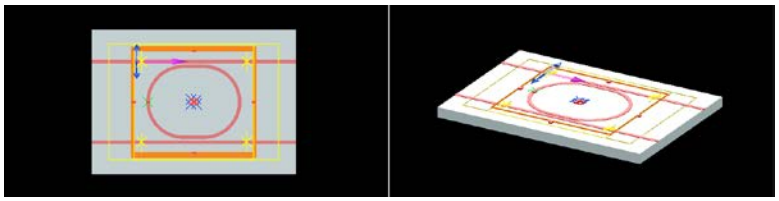

Fig. 4. Racetrack-shaped resonator view on XY and XZ axis.

3.2. Simulation

The varFDTD and FDTD algorithm were used to simulate the waveguide structure. In solving the mesh size using the FDTD method (3D FDTD) consume a long time. To overcome this problem, we used varFDTD or 2.5 D FDTD to make the simulation process easier and provide accurate results in the output of the waveguide [6]. In simulations, Lumerical software was used for FDTD analysis. Glucose solution with concentrations that vary in the range 0-180 g/L with an increase of 20 g/L used as analyte as shown in Table 2.

Table 2. Refractive index of glucose concentration in solution at λ=1550 nm (adopted from reference [3]).

Concentration (g/l)	Refractive index ($n_{g/l}$)
0	1.3101
20	1.3125
40	1.3149
60	1.3172
80	1.3196
100	1.3220
120	1.3244
140	1.3267
160	1.3291

We used various concentrations of analytes to change the background refractive index in varFDTD. In the simulation, we use a wavelength of 1550 nm, because 1550 nm is suitable for biosensing. Simulation is carried out at 300 K. The parameter that we change based on the configuration that we used in the simulation is coupling length as we know in Table 2. We analyzed transmittance on the throughport (Fig. 5) transmission device for each glucose concentration using FDTD analysis, this was done to obtain transmittance graphics for wavelengths and to obtain resonance wavelength shifts which used for calculating the sensitivity of the device.

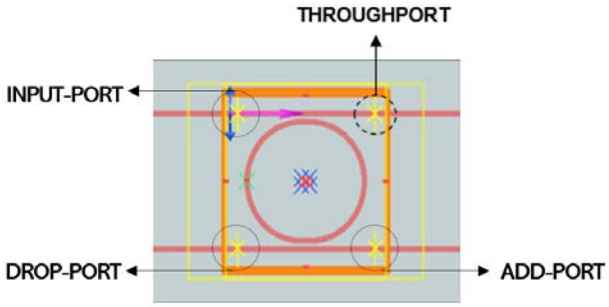

Fig. 5. Model of basic ring resonator.

4. Results and Discussion

The result of analyzing on throughport shown as Fig. 6. Figure 6 shows a graph of transmittance to the wavelength in a basic add-drop ring resonator, which on the y-axis indicating transmittance and on the x-axis indicating wavelength. Figure 6 shows that microring has multiple mode interference (MMI) [13]. We already know that for each glucose concentration has a different refractive index as shown in

Table 2. The difference in molecular concentration indicates the number of particles dissolved in different solutions (Molarity $= \frac{n}{V}$, n as a mol and V as a solvent volume). The higher the concentration of the molecule the more concentrated the solution is, the ratio between the speed of light in the air and the speed of light in the medium ($n_i = \frac{c_o}{c_m}$) defined as refractive index, so the more concentrated the speed of light in the medium is smaller, consequently the refractive index becomes greater, this is the reason for different in wavelength shift for each concentration [14, 15]. This corresponds to Eq. (5) , that the shift in resonance wavelength is linearly with to the effective index of mode [9].

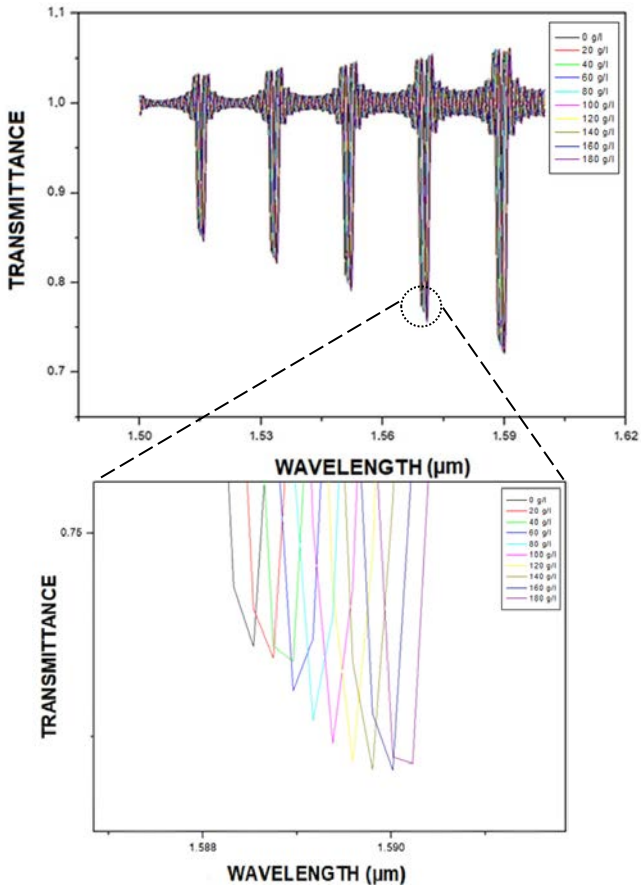

Fig. 6. MRRs Transmission response with various concentrations of glucose.

Based on the graph on Fig. 6 we can know the resonance wavelength for each concentration. Data on resonance wavelengths at each concentration we use to plot data Resonance wavelengths against the refractive index. By doing a linear fit of the plotted data obtained the sensitivity of the device is 70.32 nm/RIU as shown in Fig. 7. The model that we simulated was verified by comparing the sensitivity with the reference. The percentage of error accuracy relative to the reference = $\left|\frac{S-S_{reference}}{S_{refernce}}\right| \times 100\% = \left|\frac{70.26-65}{65}\right| \times 100\% = 8.09\%$, there is a difference between the simulation results we did with the simulation results in the reference

used by us. This is due to the different simulation methods we use. The 3D FDTD method is used to simulate the device used in the reference. we consider that using 3D FDTD takes a long time. However, the use of 2.5 FDTD in the simulations we performed can still be verified and accepted because the analysis of 2.5D FDTD still can provide accurate results. This is evidenced by the percentage of preset errors in the literature of 8.09%. So, this model appropriated with the reference and we used this model as comparison.

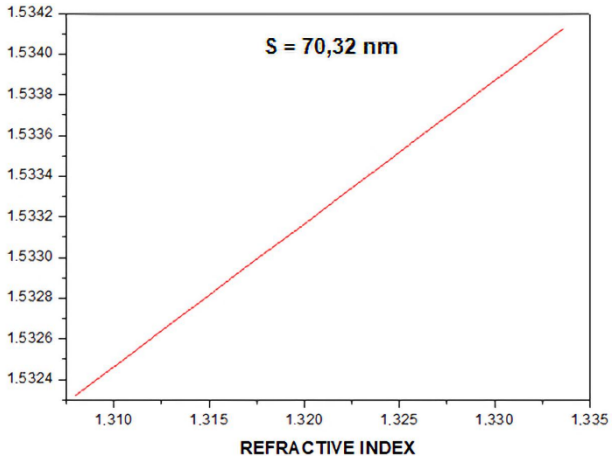

Fig. 7. Linear shift of the resonance wavelength with increasing glucose concentration.

Figure 8 shows a graph of transmittance to the wavelength in racetrack-shaped resonator. As shown in Fig. 8 the resonance wavelength shift is different from the previous configuration. This is caused by the difference of the geometry on a ring resonator so that the coupling process is different [16]. On different configurations of different wave reproduction, power transmission that reads on the various throughport [17]. The power transmission influences the Q factor, consequently, the resulting performance on different configuration is different [8].

Figure 9 shows a graph of transmittance resonance wavelength to the refractive index, which on y-axis indicates resonance wavelength and on the x-axis indicates refractive index. We can see from the Fig. 9 that model 2 (Racetrack-shaped resonators configuration) has a higher sensitivity than model 1 (Basic-add drop resonators configuration), although gradient in model 1 looks tilted than model 2. We can see the minimum and maximum value on y-axis at model 1 and model 2 is different, so the range in y-axis at model 1 and model 2 is different. Model 2 has a larger range on y-axis than model 1, this is the reason that model 2 has a higher gradient than model 1 although gradient in model 1 looks tilted than model 2. The physical reason for model 2 has a greater (S_2=79.7 nm/RIU) sensitivity because there are coupling lengths. The racetrack-shaped resonator has more control coupling coefficient [5]. The coupling efficiency is related to cavity losses, where cavity losses affect *Q*-Factor [18]. We can infer that the sensitivity can be increased by reducing cavity losses. Then racetrack-shaped configuration offers better performance than basic add-drop configuration to detect glucose.

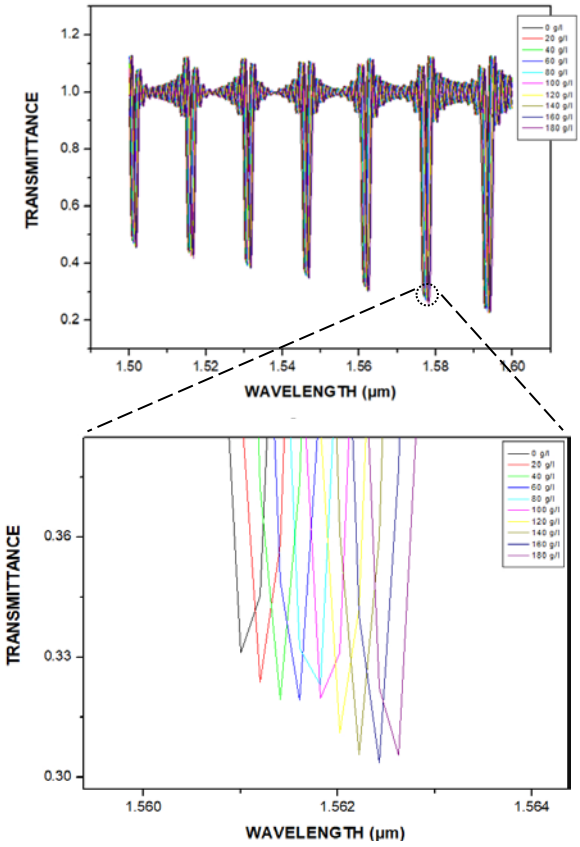

Fig. 8. MRRs Transmission response with various concentrations of glucose on racetrack-shaped resonator configuration.

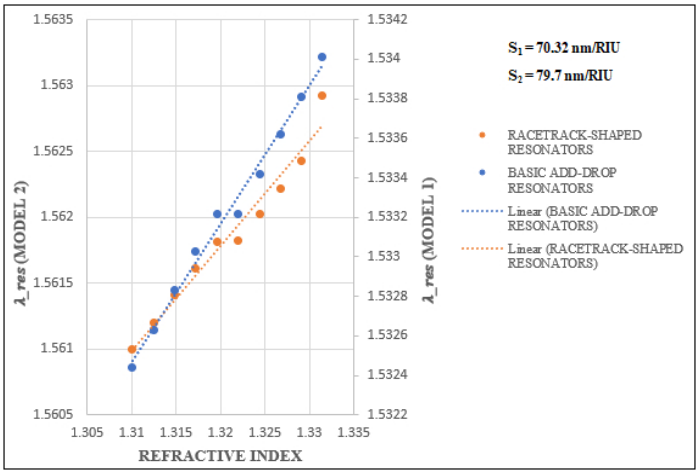

Fig. 9. Sensitivity and resonance shift of basic add-drop resonators and racetrack-shaped resonators.

5. Conclusion

Racetrack-shaped configuration is suitable for glucose sensing. Racetrack-shaped resonator (S=79.7 nm/RIU) offers better performance than basic add-drop resonator (S=70.32). The coupling length reduces losses in the cavity, so that increase the sensitivity of microring. Then racetrack-shaped configuration is better to use for glucose sensing.

Acknowledgments

A.A., C.J., and R.S. would like to thank to Universitas Pendidikan Indonesia for giving a grant for exchange student in the UPI World Class University Program.

References

1. Chen, Y.; Xianyu, Y.; and Jiang, X. (2017). Surface modification of gold nanoparticles with small molecules for biochemical analysis. *Accounts of Chemical Research*, 50(2), 310-319.
2. Sadana, A.; and Sadana, N. (2010). *Handbook of Biosensors and Biosensor Kinetics*. Elsevier.
3. Ciminelli, C.; Campanella, C.M.; Dell'Olio, F.; Campanella, C.E.; and Armenise, M.N. (2013). Label-free optical resonant sensors for biochemical applications. *Progress in Quantum Electronics*, 37(2), 51-107.
4. Mulyanti, B.; Hasanah, L.; Hariyadi, T.; Novitasari, R.; Pantjawati, A.B.; and Yuwono, H. (2015). The influence of glucose concentration to resonant wavelength shift of polymer-based microring resonators. *Advanced Materials Research*, 1112(1), 32-36.
5. Rabus, D.G. (2007). *Optical Sciences*. Springer-Verlag Berlin Heidelberg.
6. Chao, C.Y.; and Guo, L.J. (2006). Design and optimization of microring resonators in biochemical sensing applications. *Journal of Lightwave Technology*, 24(3), 1395-1402.
7. Ariannejad, M.M.; Amiri, I.S.; Ahmad, H.; and Yupapin, P. (2018). A large free spectral range of 74.92 GHz in comb peaks generated by SU-8 polymer micro-ring resonators: simulation and experiment. *Laser Physics*, 28(11), 115002.
8. Mulyanti, B.; Menon, P.S.; Shaari, S.; Hariyadi, T.; Hasanah, L.; and Haroon, H. (2014). Design and optimization of coupled microring resonators (MRRs) in silicon-on-insulator. *Sains Malaysiana*, 43(2), 247-252.
9. De Vos, K.; Bartolozzi, I.; Schacht, E.; Bienstman, P.; and Baets, R. (2007). Silicon-on-Insulator microring resonator for sensitive and label-free biosensing. *Optics Express*, 15(12), 7610-7615.
10. Mulyanti, B.; Ramza, H.; Pawinanto, R.E.; Rahman, J.A.; Ab-Rahman, M.S., Putro, W.S.; and Pantjawati, A.B. (2017). Micro-ring resonator with variety of gap width for acid rain sensing application: preliminary study. *Journal of Physics: Conference Series*, 852(1), 012043.
11. Bogaerts, W.; De Heyn, P.; Van Vaerenbergh, T.; De Vos, K.; Kumar Selvaraja, S.; Claes, T.; and Baets, R. (2012). Silicon microring resonators. *Laser and Photonics Reviews*, 6(1), 47-73.

12. Chao, C.Y.; Fung, W.; and Guo, L.J. (2006). Polymer microring resonators for biochemical sensing applications. *IEEE Journal of Selected Topics in Quantum Electronics*, 12(1), 134-142.
13. Van, V. (2016). *Optical microring resonators* (1st ed.). Boca Raton: Taylor and Francais.
14. Passaro, V.; Dell'Olio, F.; and De Leonardis, F. (2007). Ammonia optical sensing by microring resonators. *Sensors*, 7(11), 2741-2749.
15. Tan, C.Y.; and Huang, Y.X. (2015). Dependence of refractive index on concentration and temperature in electrolyte solution, polar solution, nonpolar solution, and protein solution. *Journal of Chemical and Engineering Data*, 60(10), 2827-2833.
16. Sun, L.; Yuan, J.; Ma, T.; Sang, X., Yan, B.; Wang, K.; and Yu, C. (2017). Design and optimization of silicon concentric dual-microring resonators for refractive index sensing. *Optics Communications*, 395(1), 212-216.
17. Shen, A., Qiu, C.; Yang, L.; Dai, T.; Li, Y.; Yu, H.; and Yang, J. (2015). Tunable microring based on-chip interrogator for wavelength-modulated optical sensors. *Optics Communications*, 340(1), 116-120.
18. Hazura, H.; Menon, P.S.; Majlis, B.Y.; Hanim, A.R.; Mardiana, B.; Hasanah, L.; and Wiranto, G. (2012). Modeling of SOI-based MRR by coupled mode theory using lateral coupling configuration. In *2012 10th IEEE International Conference on Semiconductor Electronics (ICSE)*. Kuala Lumpur, Malaysia, 422-425.